Peer-reviewed version available at Materials 2020, 13, 901; doi:10.3390/ma13040901

Article

Effect of Olive-Pine Bottom Ash on Properties of Geopolymers Based on Metakaolin

Eduardo Bonet-Martínez [1], Pedro García-Cobo [1]; Luis Pérez-Villarejo [2], Eulogio Castro [1,3], Dolores Eliche-Quesada [1,3]*

1. Department of Chemical, Environmental and Materials Engineering Higher Polytechnic School of Jaén, University of Jaen, Campus Las Lagunillas s/n, 23071 Jaén, Spain; ebonet@ujaen.es; pgc00002@red.ujaen.es
2. Department of Chemical, Environmental, and Materials Engineering, Higher Polytechnic School of Linares, University of Jaen, Campus Científico-Tecnológico, Cinturón Sur s/n, 23700 Linares (Jaén), Spain; lperezvi@ujaen.es
3. Center for Advanced Studies in Energy and Environment (CEAEMA) Universidad de Jaén, Campus Las Lagunillas, s/n, 23071 Jaén, Spain; ecastro@ujaen.es

*Corresponding author e-mail: deliche@ujaen.es

Abstract: In this research, the feasibility of using bottom ashes generated by the combustion of biomass (olive pruning and pine pruning) as a source of aluminosilicates (OPBA) has been studied, replacing the metakaolin precursor (MK) in different proportions (0, 25, 50, 75 and 100 wt. % substitution) for the synthesis of geopolymers. As alkaline activator an 8 M NaOH solution and a Na_2SiO_3 have been used. The geopolymers were cured 24 hours in a climatic chamber at 60 ° C in a water-saturated atmosphere, subsequently demoulded and cured at room temperature for 28 days. The results indicated that the incorporation of OPBA waste, which have 19.7 wt. % of Ca, modifies the characteristics of the products formed after alkaline activation. In general terms, the incorporation of increasing amounts of calcium-rich ashes results in geopolymers with higher bulk density. The compressive strength increases with the addition of up to 50 wt. % of OPBA with respect to the control geopolymers, contributing the composition of the residue to the acquisition of a better behaviour mechanical. The results indicate the potential use of these OPBA waste as raw material to produce unconventional cements with 28-day curing strengths greater than 10 MPa, and thermal conductivities less than 0.35 W/mK.

Keywords: geopolymers; metakaolin; biomass bottom ash; mechanical properties

1. Introduction

One of the main tasks to be addressed today by the scientific-technical community in the field of materials is the resolution of one of the energy and environmental problems caused by the massive production of greenhouse gases, as well as the deposition in landfills of the waste produced. Everyone is aware of the need to incorporate materials, whose manufacturing or processing does not involve the emission of large amounts of CO_2 into the atmosphere.

For this reason, the study and development of new cementitious materials alternative to Portland cement is a priority research line of great interest worldwide. The development of these new materials aims to minimize pollutant emissions into the atmosphere, as well as significant energy savings.

The cement industry is a highly polluting industry. One of the major problems that the cement industry presents is that during the manufacturing process, a large amount of gaseous and solid emissions such as greenhouse gases (CO_2), other polluting gases such as NO_x, SO_2 and NH_3 are generated, as well as dust. In addition, the cement manufacture implies an intense exploitation of natural resources (quarries). CO_2 emissions are mainly associated with the decarbonation of limestones, which is the main constituent of cement crude (exceeding 60 % of the total emission).

According to Singh [1] this industry faces challenges such as the growing demand for Portland cement but at the same time there are limited limestone reserves and an increase in carbon taxes.

It is estimated that between 6 % and 8 % of CO_2 emissions emitted into the atmosphere have an origin in the cement industry [2]. This industry emits between 0.7 and 1.2 tons of CO_2 per ton of clinker manufactured [2] and needs to use energy intensively during its production process. The heat required for the manufacture of the Ordinary Portland Cement (OPC) is 3100-3600 kJ/kg [3]. These numbers will not stop growing in the future, since forecasts suggest that the percentage of anthropogenic CO_2 will reach between 12-23 % by 2050 [4]. Thus, only the decomposition of calcite in Portland cement production generates 0.54 tons of CO_2, in addition to almost a ton of carbon dioxide released during the process, especially in the grinding and clinkerization stages [5]. In summary, the production of cement clinker involves the expenditure of a large amount of energy during its production, almost 810 kg of carbon dioxide (CO_2), 1 kg of sulfur dioxide (SO_2) and 2 kg are discharged into the atmosphere of nitrogen oxides (NO_x) per ton of cement produced [6-8]. Taking into account that cement production is approximately 3,700-4,000 million tons per year, this implies a substantial CO_2 footprint. . Consequently, the reduction of limestone in the raw material and, therefore, the change in its chemistry and/or the clinkerization temperature, could lead to lower CO_2 emissions.

For all the above, the cement industry faces a series of challenges for the future, such as a reduction in energy consumption and the reduction of fossil fuel consumption. Both facts would lead to a reduction in CO_2 emissions, currently the reduction energy consumption is being carried out using alternative raw materials that contain CaO in its composition, such as fly ash or blast furnace slag. In order to save fossil fuel, used tires, sewage sludge and waste from paper production are being used as alternative fuels. Another challenge of this sector is the improvement of the efficiency of the process, which would mean the implementation of technological improvements.

With this background, there is a need to develop new alternative materials to Portland cement, in whose manufacture no polluting gases are emitted and an appreciable energy savings are obtained. Among the most promising alternatives are geopolymers or materials obtained by the alkaline activation of aluminosilicates, such as natural products (clays) or industrial by-products, (glass furnace slag and/or fly ash). The raw materials after activation with alkaline solutions different binders are obtained. Geopolymers are characterized by low hydration heats, high mechanical performance, and good durability against different aggressive chemicals (acid media, sulfate attack, fire, etc.), and they do not require high consumption energy as in the manufacturing process of Portland cement. The alkaline activators used are strongly alkaline solutions (NaOH, Na_2CO_3 or hydrated alkali silicates). These alkaline materials can lead to savings in CO_2 emissions compared to Portland cements between 55-75 % [4].

Geopolymers are binders basically formed by two components: a dusty material of aluminosilicate nature that is the precursor, and an alkaline activator. The reaction processes that are carried out during the alkaline activation must be considered as a set of complex transformations of the starting solid that in its final state lead to a condensed structure with cementing properties [9-16]. These alkali-activated materials (AAM) or geopolymers, in a context of environmental degradation and due to the emphasis and widespread demand for sustainability, have increasingly attracted the attention of researchers. The growing interest in these new materials is because they can be obtained from different precursors rich in Si-Al minerals, including waste and industrial by-products, through a low temperature manufacturing process, which implies great environmental benefits compared to traditional cementing materials. Among the industrial waste most commonly used as precursors of geopolymers can be found fly ash or metal slag.

A source of aluminosilicates widely studied as a raw material in the manufacture of geopolymers with satisfactory results has been coal fly ash. However, the use of ashes from biomass sources as raw material or alkaline activator is a synthesis of geopolymers have aroused great interest among scientists. This is due to the fact that most of thermal power generation plants will be progressively closed, as a result, of fossil fuel consumption reduction policies that reduce or prevent climate change. These plants are replaced by plants that use biomass ash as a main fuel. Thus, it is

expected that by the year 2050, between one third and one half of the world's primary energy consumption will have a biomass origin [17].

The difference between coal and biomass ashes is the composition. Coal fly ashes consist mainly of iron, aluminum and silica [18], interesting elements to be used as raw material in geopolymers, since sources of silica and alumina are needed. In addition, they usually have a fairly important fraction of amorphous material, which makes them quite chemically reactive. Biomass ashes are mainly composed of silica and amorphous alumina, which is the most chemically reactive, which makes them an appropriate material to be used in the manufacture of geopolymers [19]. However biomass ashes have a higher degree of crystallinity, which makes them less reactive, especially calcium and potassium salts.

On the other hand, the olive industry, of great economic importance in the Mediterranean area, generates a large number of by-products, among which are the olive bones, the olive leaves, as well as, the pruning remains of the olive grove. The main recovery of these biomass wastes is their use as fuel for electricity generation. However, in its combustion another waste is generated, ashes. The biomass ashes generated during this process are of two types: fly and bottom ashes, the same being extracted from different stages of the combustion process. The olive biomass ashes have a high content of alkaline and alkaline earth salts, especially potassium, which makes them a priori excellent candidates to increase the pH, in the geopolymeric reaction and can substitute, if not totally, but partially, the classic alkaline activators used as sodium silicate or waterglass. Thus, according to recent research [20], ashes from the olive industry do not exhibit pozzolanic activity due to their low silica and alumina content, which prevents them from being used as Portland cement active additive. These ashes have been used, however, as partial substitutes in ceramic materials [21] and mortars [22].

Andalusia, a region located in southern Spain, has huge sources of biomass from olive grove due to the large amount of extension dedicated to this crop (1.4 million hectares) and the derived industry. The biomass potential available in this region is 3,327 kton/year [23]. This fact can give an idea of the opportunity it represents and the exploitation potential of this type of ashes to obtain geopolymeric materials. Likewise, the forestry industry constitutes another potential source of biomass. The combustion of tree pruning represents an important generation of ashes.

The objective of this work was to use bottom ash, from the combustion of biomass from olive and pine pruning, as an aluminosilicate input material to obtain alkaline-activated materials, geopolymers. Olive-pine bottom ash (OPBA) was used replacing metakaolin (MK) precursor in different amounts (0, 25, 50, 75 and 100 wt %). Their chemical, physical, mechanical and thermal properties were studied. Thus, it is intended to obtain an alternative cementitious material to Portland cement that has similar properties and at the same time a lower environmental impact.

2. Materials and methods

2.1 Raw Materials

The raw materials (Figure 1) used were metakaolin (MK), which was obtained after a calcination heat treatment at 750 °C of kaolin provided by the company Caobar S.A. located in Taracena (Guadalajara, Spain). The kaolin provided by this company had an adequate particle size, so it was not necessary to subject it to subsequent grinding treatment. Biomass bottom ashes were purchased from the Aldebarán Energía de Guadalquivir (Andújar, Jaén) and come from the calcination of biomass from the pruning of olive trees and pines. These ashes were provided with a quite heterogeneous particle size, so once received in the laboratory it was necessary to perform a grinding stage in a ball mill and finally another sieving stage until reaching a particle size of 0.150 mm.

As alkaline activator, a basic solution of 8 M sodium hydroxide was used; it was mixed with sodium silicate in aqueous medium, obtaining a pH value of 13. The sodium hydroxide was provided by Panreac SA, with a purity of 98 %. The sodium silicate solution was purchased from Panreac S.A., and has a density of 1,365 kg/cm^3 and a pH of 11.5. The composition by weight of this commercial sodium silicate is as follows: 29.2 % SiO_2; 8.9 % Na_2O and 61.9 % H_2O.

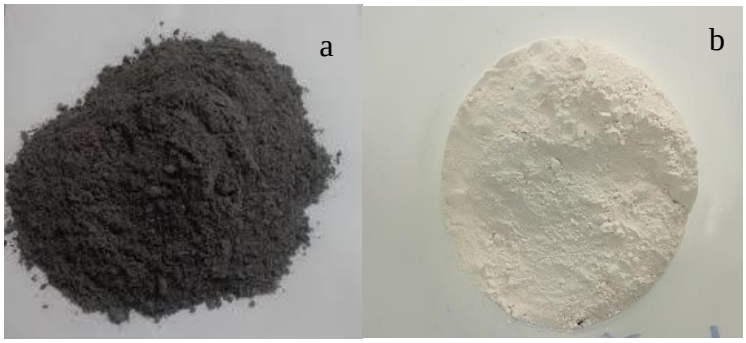

Figure 1. Pictures of raw materials: (a) olive-pine bottom ash (OPBA) after sieving stage, and (b) metakaolin after calcination step.

2.2. Raw materials characterization

A laser diffractometer Malvern Mastersizer 2000 was used to measure the particle size distribution of raw materials. This device analyzes the particle size distribution of between 0.02 and 1500 μm of any solid material dispersed in liquid medium using diffraction technology laser light.

Raw materials and geopolymers were evaluated by X-ray diffraction to know their crystalline components. The microstructural analysis was performed on a Bruker D8 Advance system with a Bruker Lineye detector at 25°C using Cu Kα radiation (λ = 1.5406 Å) at a voltage of 40 KV and an amperage of 40 mA, a range of 2θ from 5° to 60°, step 0.02°, measurement time 392 s/step. Chemical analysis of raw materials was carried out using X-Ray Fluorescence (XRF) (Philips Magix Pro equipment, PW-2440 model) a dispersive wavelength sequential spectrometer with 4 KW X-ray generator.

2.3. Preparation of MK-OPBA geopolymers

The alkaline activating consists of a solution of sodium hydroxide and sodium silicate. First, an 8 M sodium hydroxide solution is prepared (80 g of NaOH are dissolved in 195 g of water), to which the appropriate amount of sodium silicate (300 g) is added continuously and slowly. The entire mixing process is carried out on a magnetic stirrer with an approximate duration of ten minutes. After stirring, the mixture is allowed to cool to room temperature. The alkaline activator solutions are finally subjected to a pH measurement. These pH measurements were made with a Crison Basic 20 pH meter. In all series, the activating solution has remained constant, as well as the solid / liquid ratio = 1.18.

The formed geopolymers are prepared by replacing different weight ratios of MK precursor (0, 25, 50, 75 and 100 wt %) by the olive-pine bottom ash residue. The control geopolymers contain only as a source of aluminosilicate, MK (0 % OPBA).

The necessary quantities of MK and the OPBA residue (Table 1) are weighed and mixed five minutes in solid state in a planetary kneader until a homogeneous solid mixture is achieved. After this time, the activator solution is added slowly, reaching a time of pouring and mixing slowly of two minutes. Then the kneading is raised at rapid speed mixing for another ten minutes, thus achieving 17 minutes of mixing for each series of geopolymers.

Table 1. Quantities of raw materials and, Si/Al and Si/Na molar ratio of synthesized geopolymers

MK (wt %)	OPBA (wt %)	Si/Al molar ratio	Si/Na molar ratio	MK (g)	OPBA (g)
100	0	1.63	0.42	450.0	0

75	25	1.91	0.44	337.5	112.5
50	50	2.32	0.46	225.0	225.0
25	75	3.05	0.49	112.5	337.5
0	100	4.62	0.52	0	450.0

Once the kneading has been carried out, the geopolymeric mixture is poured onto polyethylene containers, slowly and providing small blows to achieve a better compaction of the geopolymer in the mold. The containers are covered with a plastic film, thus ensuring that the amount of water lost in the geopolymer mixture is the minimum. Subsequently, the molds are transferred to the climatic chamber where they are cured at 60 ° C with a water saturated atmosphere for 24 hours. The geopolymer precursors are then demoulded and cured at room temperature for 28 days.

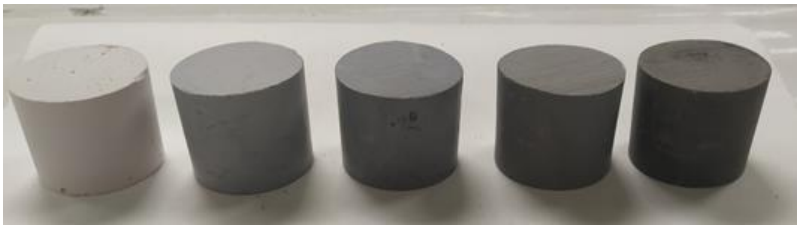

Figure 2. The geopolymers obtained, from left to right: 0 wt % OPBA, 25 wt % OPBA, 50 wt% OPBA, 75 wt % OPBA and 100 wt % OPBA.

The geopolymers were designated as *xMK-yOPBA* where *x* denotes the MK content (wt. %) and y the OPBA wt. % content. It can be seen in Table 1 that as the amount of substitution of MK by OPBA increases, the Si / Al molar ratio increases, while the Na / Si molar ratio remaining practically constant.

2.4. Characterization of MK-OPBA geopolymers

The bulk density determination was carried out according to the UNE-EN 772-13, 2001 Standard [24]. Water absorption was determined according to ASTM C373 standard [25].

Mechanical properties of geopolymers were conducted by measuring compressive strength. This assay was carried out according to the standard procedure UNE-EN-772-1, 2011 [26] using a Material Test System (MTS) 810 Material Testing Systems laboratory press. The geopolymers were tested by applying a progressively increasing load to the center of their upper surface until failure. Compressive strength of geopolymeres is obtained by dividing the maximum load by the average surface area of the two bearing surfaces with an accuracy of 0.1 MPa.

Thermal conductivity of the alkali-activated materials was determined at 10 °C using a FOX 50 Heat Flow Meter (TA Instruments) in accordance with ISO 8302, 1991 [27].

An equipment of attenuated total reflectance (ATR-FTIR) Fourier Transform Infrared spectroscopy Vertex 70 equipment from Bruker was used to characterize the geopolymers.

Microstructural and porosity features were examined by means of scanning electron microscopy (SEM) using a JEOL equipment, SM 840 model and assisted by Energy dispersive X-ray Spectroscopy (EDS). Samples were placed on an aluminum grate and coated with carbon using the JEOL JFC 1100 sputter coater.

3. Results and discussion

3.1. Raw materials characterization results

Table 2 shows the chemical composition of raw materials, the MK and the OPBA waste determined by XRF. The MK is composed almost entirely of silica (58.03 %) and alumina (40.29 %).

The OPBA waste have a high silica content (46.10 %), at the same time presenting high content in calcium oxide (19.65 %) and alumina (12.04 %). Other oxides such as magnesium oxide (3.71 %), potassium oxide (4.59 %) or iron oxide (4.78 %) are also significant. The loss of ignition(LOI). is of 5.58 wt %. The sum of SiO_2 and Al_2O_3 in the OPBA waste accounts for 58wt %. Therefore OPBA waste are a good candidate for the substitution of MK in the synthesis of geopolymers.

Table 1. Chemical composition of olive-pine bottom ash (OPBA) and metakaolin (MK) raw materials

Oxide content (%)	OPBA	MK
SiO_2	46.10	58.03
Al_2O_3	12.04	40.29
Fe_2O_3	4.78	0.42
CaO	19.65	0.09
MgO	3.71	0.11
MnO	0.09	0.01
Na_2O	0.78	0.02
K_2O	4.59	0.39
TiO_2	0.83	0.15
P_2O_5	1.12	0.07
SO_3	0.41	0.01
LOI	5.58	0.36

The mineralogical composition of MK determined by XRD indicate that the precursor presents quartz as the only crystalline phase (Figure 3). The halo observed between 2 theta 20-30 º is mainly attributed to the degree of amorphousness of the precursor. The OPBA waste diffraction pattern (Figure 3) indicates that biomass bottom ashes are mainly composed of silica and calcium carbonate. Also presenting a large number of small diffraction peaks corresponding to calcium oxide and some aluminosilicates, according to the XRF data (Table 1).

Peer-reviewed version available at Materials 2020, 13, 901; doi:10.3390/ma13040901

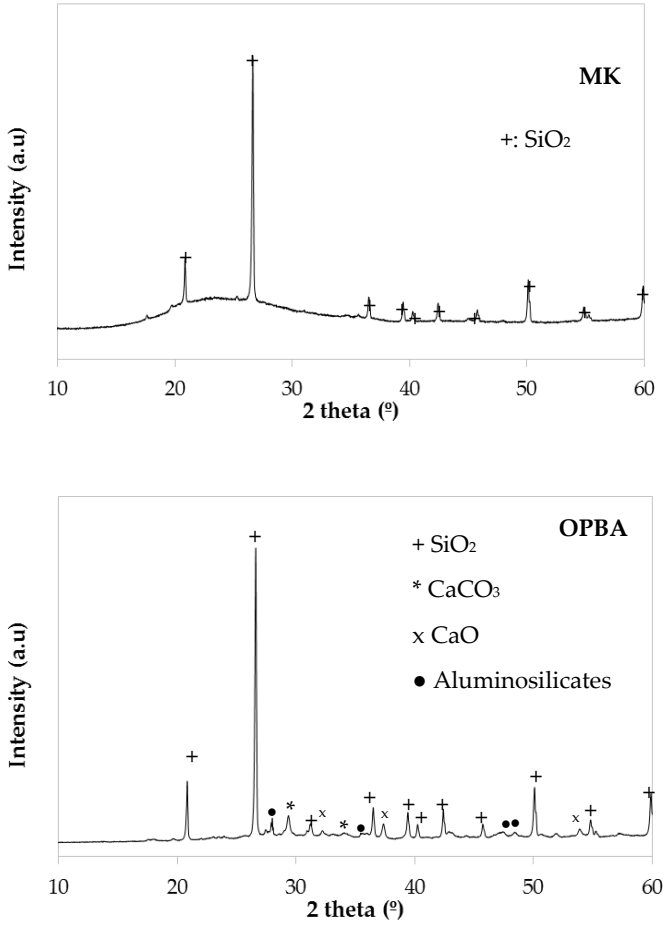

Figure 3. XRD patterns of raw materials: metakaolin (MK) and olive-pine bottom ash (OPBA)

The particle size distribution of the precursors MK and OPBA is shown in Figure 4. The particles present in the MK precursor were thinner than those present in the OPBA waste. The average particle size D_{50} is 9.6 µm for the MK and 52.6 µm for the OPBA waste (Figure 4).

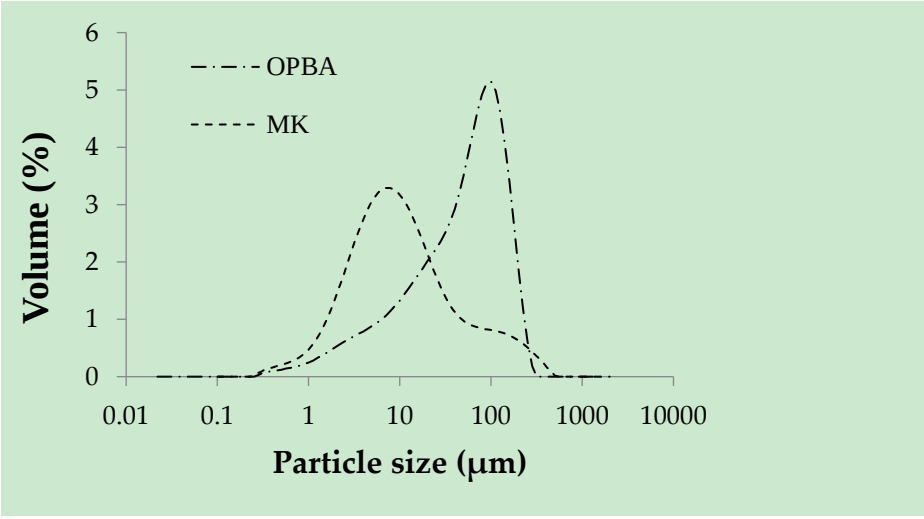

Figure 4. Particle size distribution of raw materials: metakaolin (MK) and olive pine bottom ash (OPBA).

Peer-reviewed version available at *Materials* **2020**, *13*, 901; doi:10.3390/ma13040901

The MK is made up of particles of a similar size to the silt (79.0 %), while the OPBA waste have higher percentage of sand-sized particles (51.5 %), presenting a lower percentage of particles of silt size (33.3 %) (Table 2). The particles present in the precursor MK are smaller than the OPBA waste particles.

Table 2. Particle size distribution of MK and OPBA waste.

Particle size distribution (mm)	MK (%)	OPBA (%)
Clay content < 0.002	8.13	15.25
Silt content (0.002-0.063)	78.98	33.25
Sand content (0.063-2)	12.89	51.51

Micrographs obtained by Scanning Electron Microscopy (SEM) and EDS analysis corresponding to the raw materials MK precursor and the OPBA waste can be observed in Figure 5.

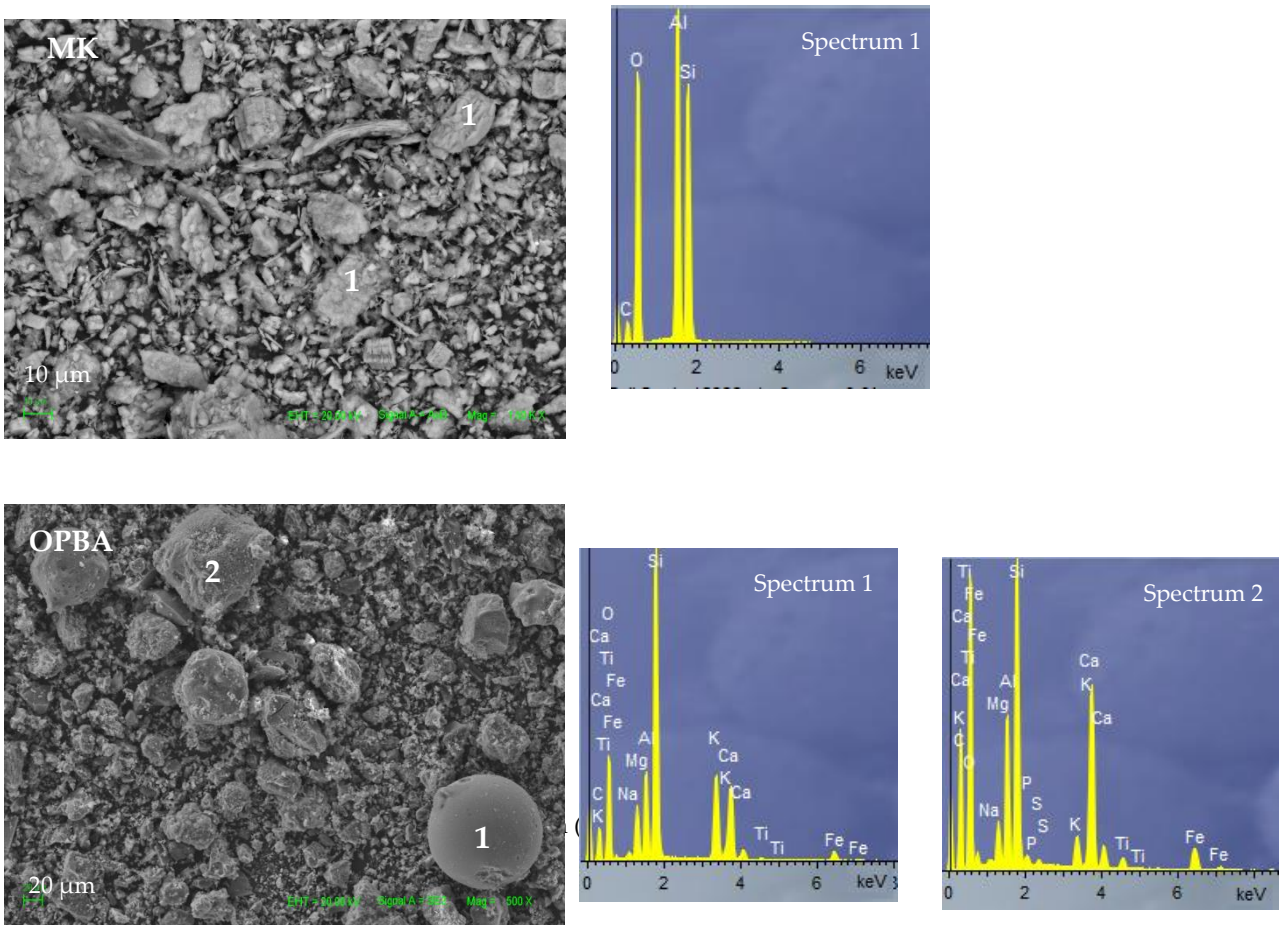

Figure 5. SEM-EDS of raw materials apractice metakaolin (MK) and olive-pine bottom ash (OPBA)d.

The MK and OPBA have a heterogeneous structure with a widespread particle size distribution. The OPBA particles are larger than MK particles, according to the particle size distribution data. The MK particles have morphology of deformed flakes all rich in Si and Al, the main constituents of MK. The biomass bottom ashes present two types of particles, spherical and acicular particles. Both particles are rich in Si, Al, Ca, Mg and K, being the richest in calcium acicular particles.

3.2. MK-OPBA geopolymers characterization results

3.2.1. FTIR of MK-OPBA geopolymers

In the hardening process of the xMK-yOPBA geopolymers, a series of chemical bonds are formed as a consequence of the chemical reactions that occur once the activating solution is added to the mixture. These chemical bonds can be observed by FTIR. Figure 6 shows the FTIR spectra of the geopolymers after 28 days of curing. As a comparison, the FTIR spectra of the MK and OPBA raw materials are also shown. In the raw materials MK and OPBA a band centered at 1058 cm^{-1} a or 987 cm^{-1}, respectively characteristic of the stretching modes of the T-O-T bond, where T can be Si or Al. can be observed. This band, with the incorporation of the activating solution, shows a shift towards lower wavenumbers (974 - 945 cm^{-1}) for geopolymers containing between 0-100 wt. % of OPBA. The displacement observed can be associated with the dissolution of the aluminosilicate source. This displacement indicates that the silicate group has geopolymerized forming the geopolymeric gel. The displacement of the band towards greater wavelengths as the percentage of OPBA decreases, could be influenced by a lower availability of calcium in the specimens. The presence of the N-A-S-H gel has a greater preponderance on the appearance of the second gel, (N, C)-A-S-H, whose formation is subsequent due to the incorporation of a greater amount of calcium [28]. The band that appears at 796 cm^{-1} on the MK precursor can be assigned to bending of the Si-O-Si bonds in the network of the unreacted silica [29]. In the region between 3800 and 1400 cm^{-1} two bands can be observed. The first very wide band centered between 3369-3342 cm^{-1} is attributed to the vibration of the –OH bond of the molecular water present freely or physically absorbed on the surface or pores of the gel [30]. The second band centered between 1650-1644 cm^{-1} corresponds to the vibration by deformation of the H-OH bond, since the high alkali content in the pore solution prevents evaporation of the water [31]. The greater intensity of these bands as increasing amounts of ash are incorporated as raw material, can be attributed to the greater number of water molecules present in the geopolymer as the SiO_2/Al_2O_3 ratio increases [32], as well as to a lower degree of geopolymerization reaction for ash contents greater than 50 wt. %, since water is consumed during the different reaction stages. In the region between 1400-900 cm^{-1}, in addition to observing the bands centered at 974-945 cm^{-1} associated with the asymmetric stretching vibrations of the Si-O-Si and Si-O-Al bonds of the geopolymeric gel formed, another band centered between 1409-1381 cm^{-1} can be observed that corresponds to the asymmetric tension vibrations of the CO bonds indicating the presence of sodium carbonates (CO_3^{2-}). This bands is complemented by a shoulder band centered at 877-793 cm^{-1} that corresponds to the vibration by symmetric deformation of the O–C–O bonds. The bands present in the region between 800-600 cm^{-1} are related to the stretching vibration of the Al-O bonds, specifically for Al ions with coordination 4. Another band located at 880 cm-1 should be assigned to Si-O-M in the asymmetric stretching mode [30].

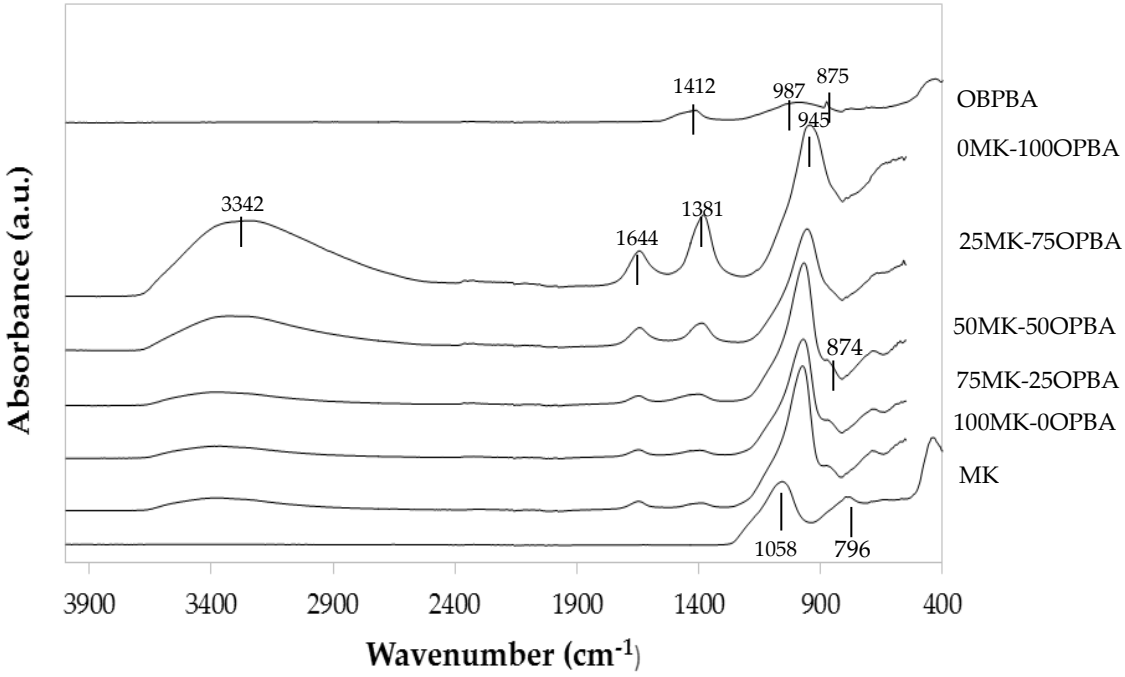

Figure 6. FTIR spectra of raw materials: MK and OBPBA and geopolymers xMK-yOPBA

3.2.2. XRD of MK-OPBA geopolymers

Figure 7 shows the diffractograms of the synthesized geopolymers and, as a comparison, the diffractograms of the raw materials, MK and OPBA. The presence of a series of diffraction peaks present in the raw materials that indicates the presence of crystalline substances that are not involved in the geopolymerization reaction can be observed. These peaks are less intense, indicating that the surface of the crystals is attacked in the geopolymerization reaction due to the aggressive medium in which they are found. No new crystalline phases appearing in the geopolymerization process. The diffraction peaks of the quartz, present in both raw materials the MK and the OPBA, or the calcium carbonate and calcium oxide present in the OPBA are observed. The presence of amorphous substances can also be observed, due to the deviations observed in the baseline with respect to the raw material MK between the values of 2θ between 20° and 35° (Figure 7). This halo can be observed more accurately in Figure 8. This fact could indicate the appearance during the geopolymerization reaction of an amorphous geopolymeric gel as indicated FTIR data.

Peer-reviewed version available at Materials 2020, 13, 901; doi:10.3390/ma13040901

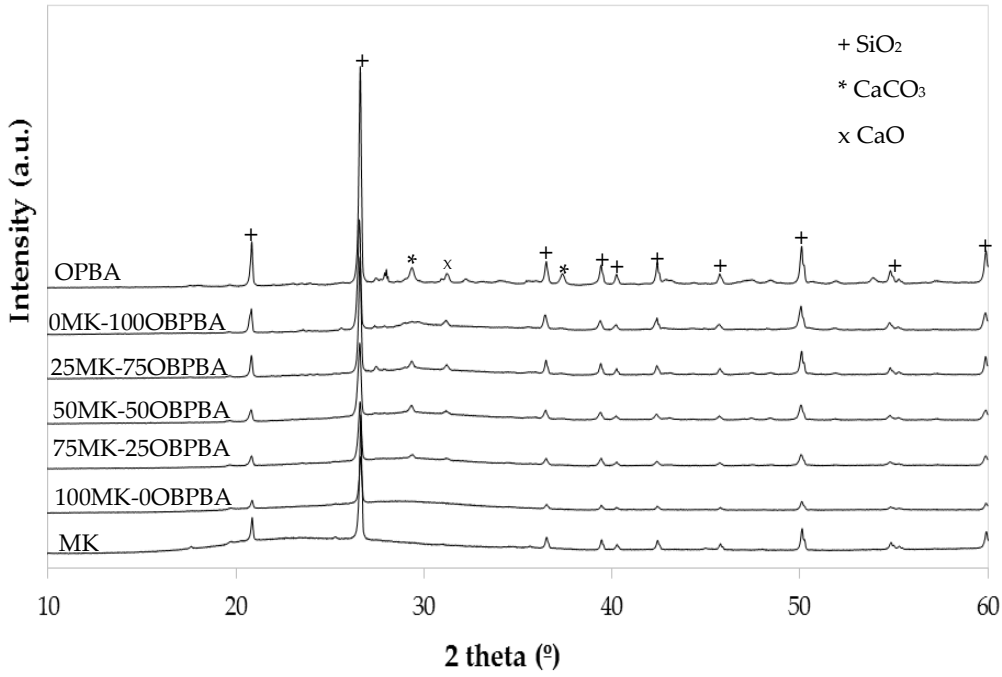

Figure 7. XRD patterns of raw materials MK and OPBA and the geopolymers xMK-yOPBA

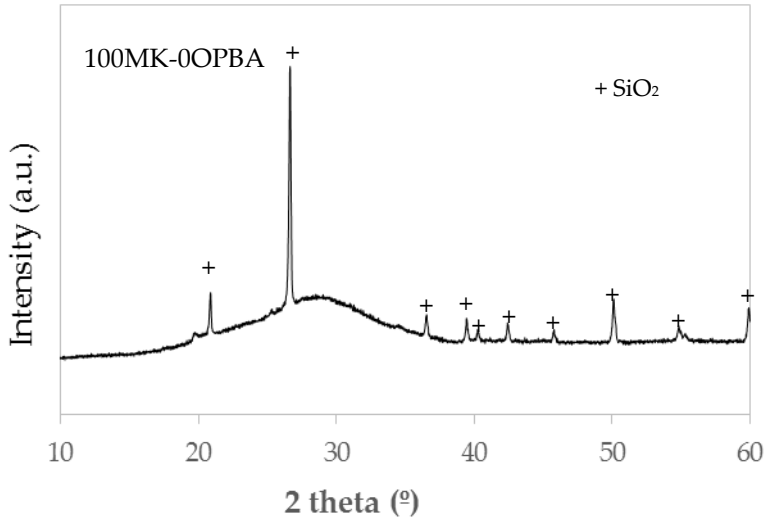

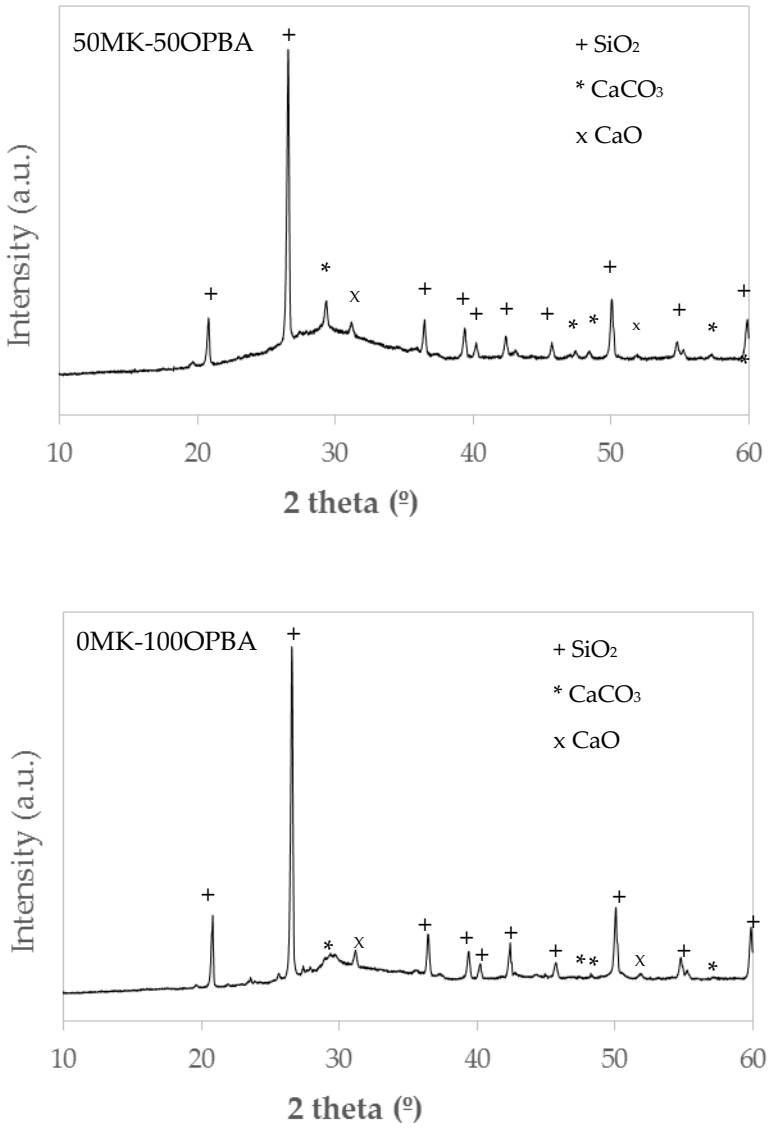

Figure 8. XRD patterns of 100MK-0OPBA, 50MK-50OPBA and 0MK-100OPBA geopolymers.

3.2.3. Bulk density, apparent porosity and water absorption of MK-OPBA geopolymers

The data of bulk density of the different OPBA geopolymers after 28 days of curing are shown in Figure 9. The bulk density of the control geopolymer 100MK-0OPBA is 1251 kg/m^3. The replacement of 25-50 wt. % of OPBA by MK produced a slight increase in bulk density, up to 1268 kg/m^3 for the 50MK-50OPBA geopolymers. The addition of 75-100 wt. % of OPBA waste produced a remarkable change in the bulk density increasing up to 1407 kg/m^3 for geopolymers containing only OPBA (0MK-100OPBA). The real density of the OPBA, 2546 kg/m^3, is lower than the real density of the MK, 2631 kg/m^3. Therefore, the increase in the bulk density of MK-OPBA geopolymers may be due to OPBA waste, which acts as microfillers; this produces an increase in the bulk density of the specimens as a denser microstructure is formed, mainly due to the geopolymerization reactions of the OPBA waste caused by the calcium content, similarly at the effect produced on thebulk density of the cement paste by other supplementary materials, such as silica fume, fly ash and granulated blast furnace slags [33].

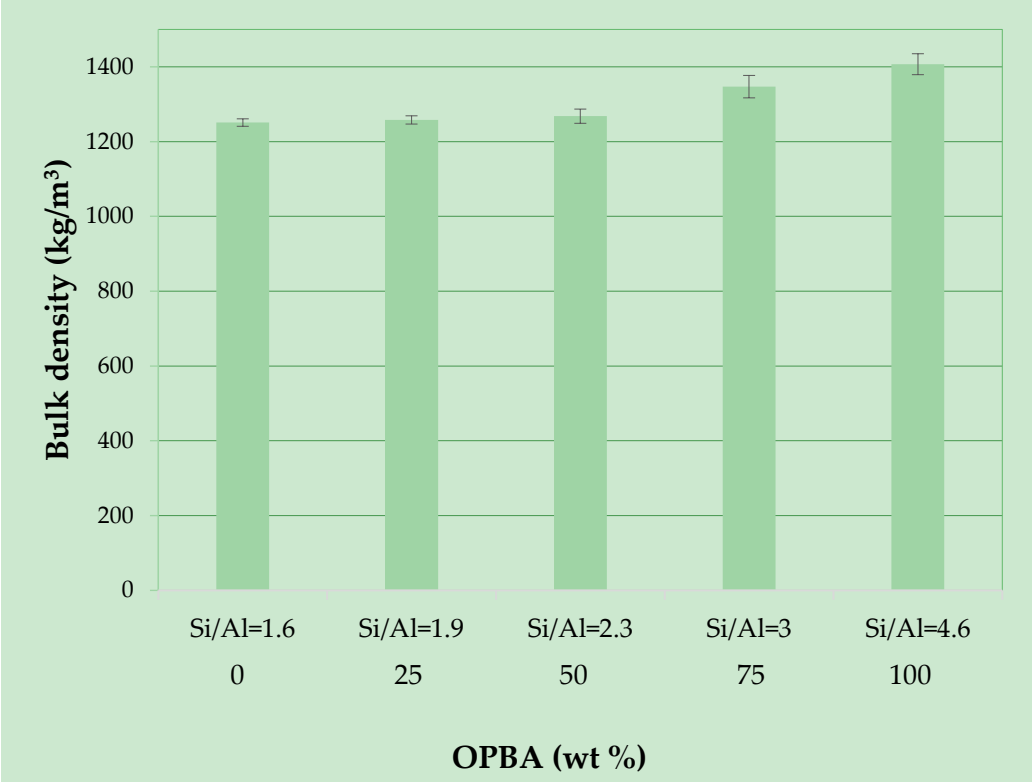

Figure 9. Bulk density of the MK-OPBA geopolymers after 28 days of curing as function of the OPBA waste content and the Si/Al molar ratio.

The porosity of geopolymers to be used as building materials makes them vulnerable to weathering and chemical attack. Control geopolymers and specimens containing up to 50 wt. % of OPBA have low bulk density and high apparent porosities between 41-39 % for control samples (100MK-0OPBA) and 50MK-50OPBA geopolymers, respectively. As observed in bulk density, the addition of larger amounts of bottom ash (75-100 wt. %) produced a more pronounced decrease in apparent porosity up to 20 % for geopolymers that use only OPBA waste (0MK-100OPBA) as raw material (Figure 10). This fact could be due to the interpenetrating action and the filling effect of biomass bottom ashes. The water absorption, an indirect measure of the open porosity of geopolymers, follows the same trend as the apparent porosity. Control and geopolymers containing up to 50 wt. % of OPBA waste have similar water absorption values, between 32.8 % for 100MK-0OPBA and 31.0 % for 50MK-50OPBA specimens. The incorporation of 75-100 wt. % of OPBA waste produced a more pronounced decrease to 14.7 % for 0MK-100OPBA geopolymers (Figure 10).

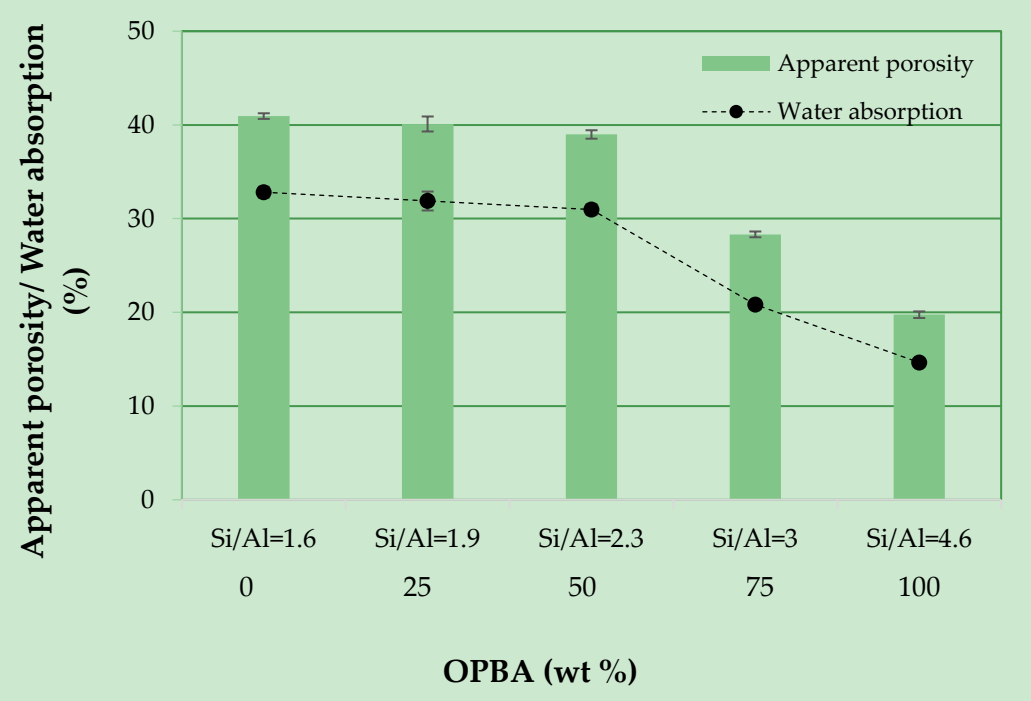

Figure 10. Apparent porosity and water absorption of the MK-OPBA geopolymers after 28 days of curing as function of the OPBA waste wt. % content and the Si/Al molar ratio.

3.2.4. SEM study of MK-OPBA geopolymers

The microstructure of the specimens is shown in Figure 11 through the SEM micrographs of geopolymers after 28 days of curing. The formation of the geopolymeric gel in all samples can be observed. In the 100MK-0OPBA control geopolymers, the sodium aluminosilicate hydrate (N-A-S-H) gel is observed by EDS. The presence of calcium in the biomass bottom ashes promotes the formation of other types of products, mainly aluminium-modified calcium silicate hydrate (C-A-S-H) gel, with a different kinetics and reaction degree to the N-A-S-H geopolymer gel [34]. The EDS analysis of the 50MK-50OPBA and 0MK-100OPBA geopolymers indicates the coexistence of the two C-A-S-H and N-A-S-H gels, the latter containing small amounts of calcium (N, C)-A-S-H. This is due to the significant amount of calcium present in the OPBA waste. The appearance of the gel (N, C) -ASH is later than that of NASH, because calcium ions, together with those of aluminum, diffuse through the cementitious matrix formed. Thus, a small number of calcium ions interact with the N-A-S-H gel to form the gel (N,C)-A-S-H. The appearance of these two gels is indicative of the formation of the geopolymer [28]. These products, in general, have a positive effect on the mechanical strength of the material [35, 36]. The geopolymers have a denser structure as larger amounts of biomass bottom ash are added, according to the bulk density data. Spherical voids, due to air bubbles during the geopolymerization process can be observed. Also, fracture microcracks generated both by the retraction of the material, which is characteristic in geopolymer systems with high SiO_2/Al_2O_3 ratios [34] are also visible. The microcracks are larger in the geopolymer sample that uses only OPBA as raw material (0MK-100OPBA). In the samples incorporating OPBA waste as raw material, the presence of OPBA particles that have not reacted and that are embedded in the gel of the products formed can be observed. These particles of OPBA exhibit a spherical shape with the growth of some reaction products on the surface or partial dissolution of the outer layer [37]. The 0MK-100OPBA geopolymers present a greater amount of unreacted residue, resulting in a smaller amount of geopolymeric gel formed in accordance with XRD and FTIR data.

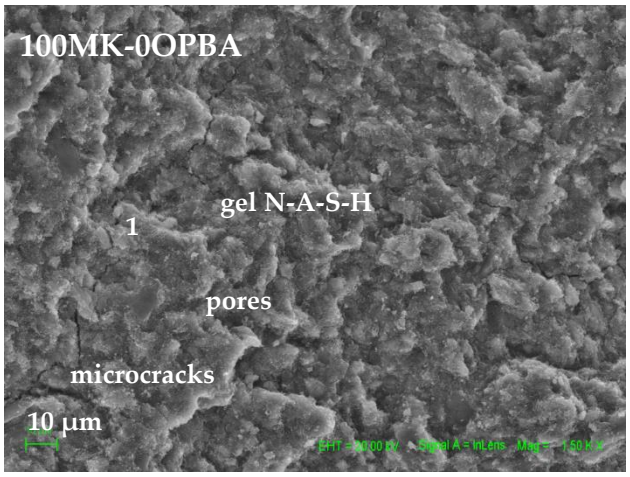

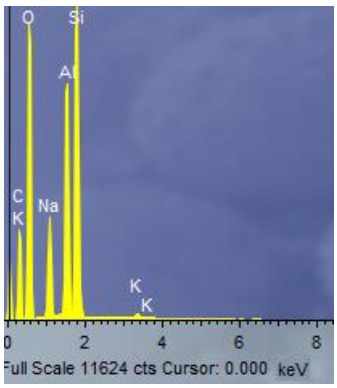

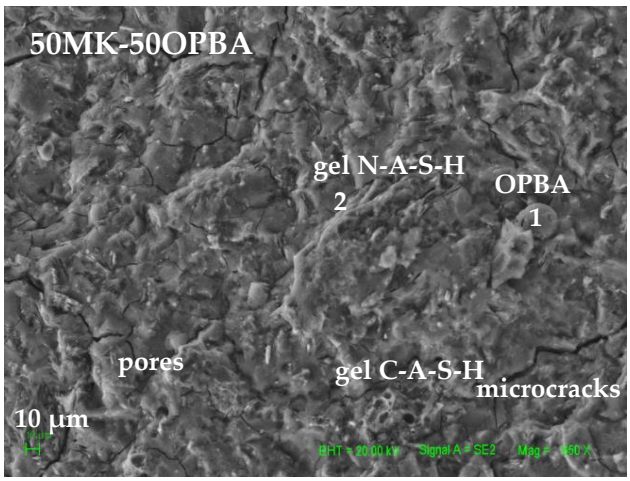

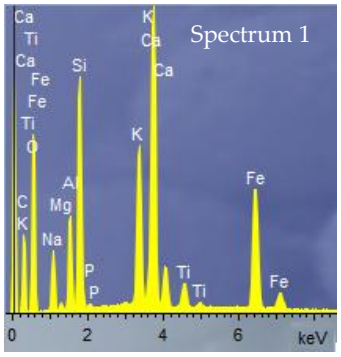

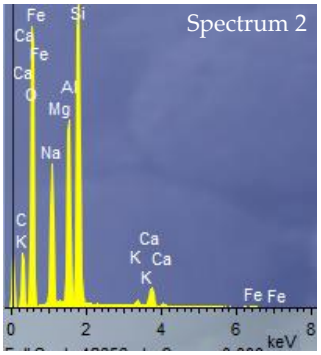

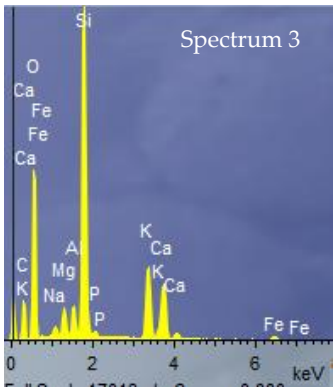

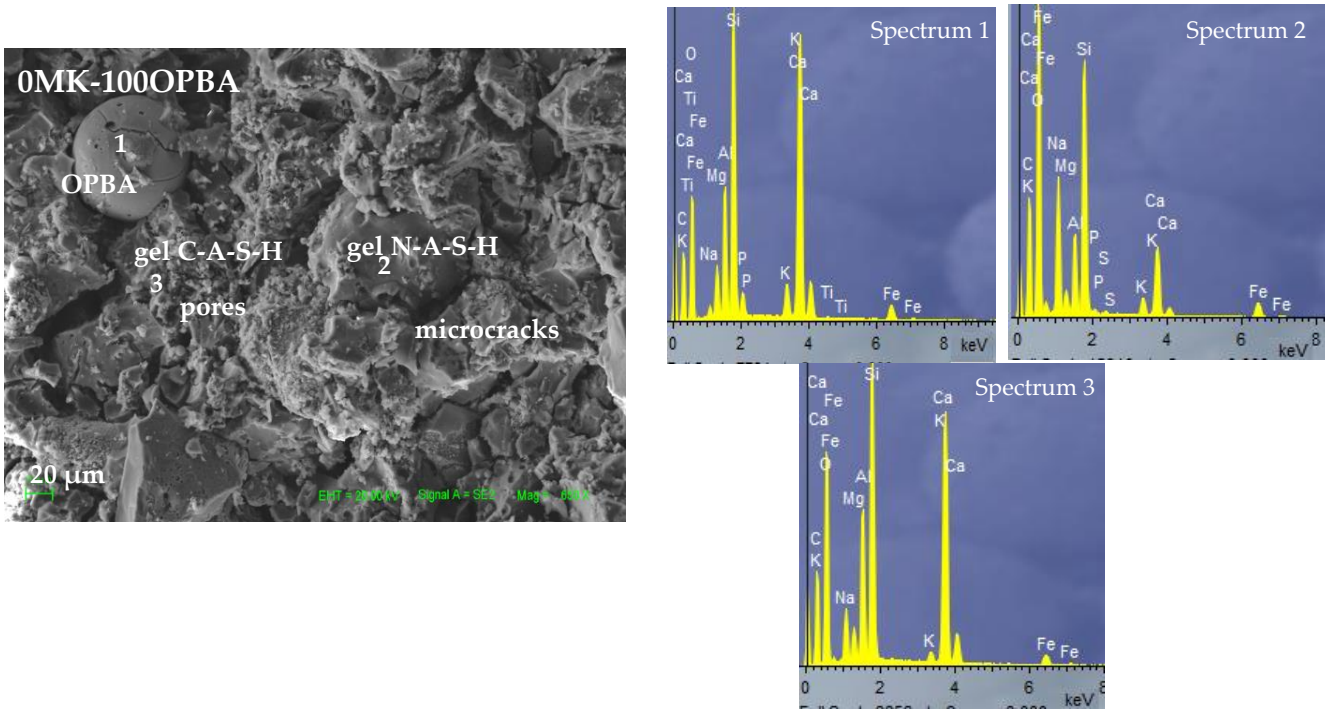

Figure 11. SEM micrographs and EDS analysis of 100MK-0OPBA, 50MK-50OPBA and 0MK-100OPBA geopolymers after 28 days of curing.

3.2.5. Compressive strength of MK-OPBA geopolymers

The compressive strength of geopolymers is shown in Figure 12. The compressive strength of the control geopolymers 100MK-0OPBA is 23 MPa. The incorporation of up to 50 wt. % of OPBA waste produced an increase in compressive strength, obtaining a maximum value of 40.1 MPa for the 50MK-50OPBA geopolymers. The incorporation of OPBA waste, which contains calcium, leads to the formation of other types of structures, as indicated by the SEM-EDS data, generate mechanical strength increases. Therefore, the increase in mechanical strength in geopolymers containing up to 50 wt. % of OPBA can be attributed to the coexistence of N-A-S-H gel obtained after MK activation, together with C-N-A-S-H gels formed after activation OPBA waste [38, 39]. The addition of 75 wt. % and 100 wt. % of bottom ash biomass, 25MK-75OPBA and 0MK-100OPBA geopolymers, despite presenting a more compact structure, with higher bulk density and lower porosity, due to the greater incorporation of the source of calcium, have lower values of compressive strength, 18.5 and 11.6 MPa for 25MK-75OPBA and 0MP-100OPBA geopolymers, respectively. This decrease in mechanical properties may be attributed to the larger size of the visible microcracks, that propagate through the matrix easily, as well as the smaller amount of geopolymer gel formed and the greater amount of unreacted ashes, which leads to geopolymers with less mechanical strength due to these defects in the microstructure as indicated SEM micrograph and XRD and FTIR data.

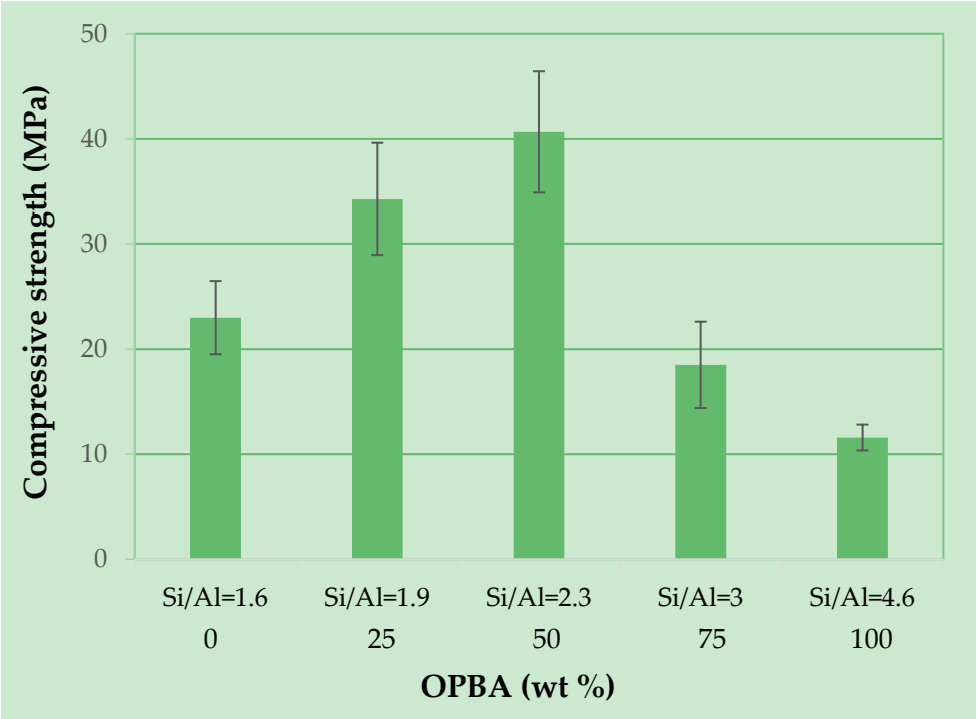

Figure 12. Compressive strength of the MK-OPBA geopolymers after 28 days of curing as function of the OPBA waste wt. % content and the Si/Al molar ratio.

3.2.6. Thermal conductivity of MK-OPBA geopolymers

The thermal conductivity data at 10 °C of the geopolymers after 28 days of curing can be seen in Figure 13. The thermal conductivity of the control geopolymers (100MK-0OPBA) is 0.22 W/mK, increasing as higher amounts of OPBA waste are substituted by MK, up to 0.31 W/mK for geopolymers containing as raw material only biomass bottom ashes (0MK-100OPBA specimens). These results are in agreement with the bulk density data, with the denser geopolymers having a lower thermal insulation capacity. However, the 50MK-50OPBA geopolymers have a thermal conductivity of 0.26 W/mK, which represents a slight increase of this property with respect to the control geopolymers. When comparing thermal conductivity values of common building materials as: concrete block (0.7-0.8 W/mK), common ceramic brick (0.4-0.8 W/mK) and Portland cement-based concrete (0.7-2.6 W/mK), it can be seen that experimental MK-OPBA geopolymers show superior thermal isolation to common building materials. Therefore, geopolymers synthesized using as raw materials MK and OPBA waste under the established synthesis conditions have low thermal conductivity.

Peer-reviewed version available at Materials 2020, 13, 901; doi:10.3390/ma13040901

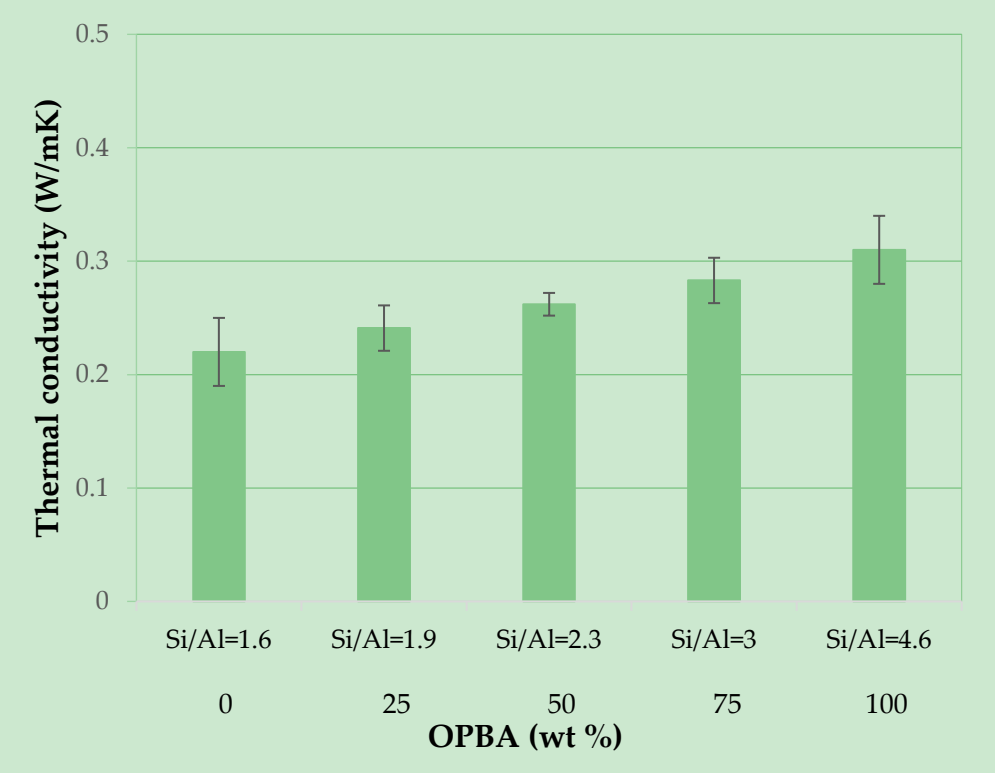

Figure 13. Thermal conductivity of the MK-OPBA geopolymers after 28 days of curing as function of the OPBA waste wt. % content and the Si/Al molar ratio.

4. Conclusions

The results obtained in this work reveal the potential use of OPBA with high calcium content (19.7 wt. %) as a precursor in the manufacture of metakaolin-based geopolymeric materials. Alkaline activation of precursors with Si/Al and Na/Si molar ratios between 1.63-4.63 and 0.42-52 ranks, respectively were obtained. The OPBA raw material allowed the obtaining of materials with cementing characteristics that can acquire maximum compressive strength of up to ~ 40 MPa with 28 days of curing (50MK-50OPBA geopolymers). The incorporation of calcium-rich ashes resulted in a denser and more compact structure, as well as the formation of other types of cementitious products, which contributes to the increase in mechanical performance until the incorporation of up 50 wt. % of OPBA waste. The addition of greater OPBA incorporations (75-100 wt. %) results in geopolymers with worse mechanical properties, possibly due to the lower amount of geopolymeric gel, higher amount of unreacted ash and the formation of larger microcracks in the matrix. The thermal conductivity increases with the replacement of increasing amounts of OPBA waste by MK precursor according to the bulk density data. However, all synthetized geopolymers have low values of thermal conductivity, between 0.22 and 0.31 W/mK, so the specimens have high thermal insulation capacity. Therefore, it is possible to obtain geopolymers by replacing the precursor MK with the OPBA waste with adequate physical, mechanical and thermal properties. The incorporation of 50 wt. % of OPBA waste results in geopolymers with better mechanical properties. These new construction materials can be used as substitutes for materials whose economic and environmental cost is much higher when they are produced, such as Portland cement.

Author Contributions: E.B.M. did part of the experimental work in the laboratory, P.G.C. did part of the experimental work in the laboratory. LPV writing—original draft preparation. E.C. review the manuscript. D.E.Q. did some test, writing—review, editing and designed the research. L.P.V., E.C. and D.E.Q. critically discussed the results

Funding: This research was funded by FEDER/Ministry of Science, Innovation and Universities, State Research Agency

Acknowledgments: This work has been funded by the project *Development and characterization of new geopomerical composites based on waste from the olive industry. Towards a sustainable construction* (MAT2017-88097-R), FEDER / Ministry of Science, Innovation and Universities, State Research Agency. The authors thank "Caobar S.A." company and Aldebarán Energía del Guadalquivir S.A. for supplying the kaolinite and biomass bottom ash, respectively. Technical and human support provided by CICT of Universidad de Jaén (UJA, MINECO, Junta de Andalucía, FEDER) is gratefully acknowledged.

Conflicts of Interest: The authors declare no conflict of interest.

References

[1] Singh, B. Ishwarya, G. Gupta, M. Bhattacharyya, S.K. Geopolymer concrete: A review of some recent developments. *Constr. Build. Mater*. **2015**, 85, 78-90.

[2] Goñi, S. Guerrero, A. Hydraulic activity of belite cement from class C coal fly ash. Effect of curing and admixtures. *Mater. Construcc*. **2006**, 56, 61-77.

[3] Popescu C.D. Muntean M. Sharp J.H. Industrial trial production of low energy belite cement. Cement and Concrete Composites. **2003**, 25, 689-693.

[4] Font, A. Soriano, L. Moraes-Pinheiro, S.M. Tashima, M.M. Monzó, J. Borrachero, M.V. Payá, J. Design and properties of 100% waste-based ternary alkali-activated mortars: Blast furnace slag, olive-stone biomass ash and rice husk ash. *J. Clean. Prod*. **2020**, 243,118568.

[5] de la Torre, A.G. Aranda, M.A.G. de Aza, A.H. Pena, P. de Aza, S. Belite Portland Cements. Synthesis and Mineralogical analysis. *Bol. Soc. Esp. Ceram*. V. **2005**, 44, 185-191.

[6] Habert, G. d'Espinose de Lacaillerie, J.B. Roussel, N. An Environmental evaluation of geopolymer based concrete production: reviewing current research trends. *J. Clean. Prod*. **2011**, 19, 1229-1238.

[7] Van den Heede, P. De Belie, N. Environmental impact and life cycle assessment (LCA) of traditional and "Green" concretes: literature review and theoretical calculations. *Cement Concrete Comp*. **2012**, 34, 431-442.

[8] Bhutta, A. Farooq, M. Zanotti, C, Banthia, N. Pull-out behavior of different fibers in geopolymer mortars: effect of alkaline solution concentration and curing. *Mater. Struct*. **2017**, 50, 1-13.

[9] Glukhovskiy, V.D. Soil silicates. Gosstroy publsh, Kiev (1959). (in Russian).

[10] Glukhovskiy, V.D. Soil-Silicate Articles and Constructions. Kyiv, Budivelnik publish, (1967). (in Ukrainian).

[11] Krivenko, P.V. Alkaline Cements. Proceed. First Intern. Conf. "Alkaline cements and Concretes". Kiev, Vipol publish, pp.11-129, (1994).

[12] Krivenko, P.V. Alkaline Cements: Terminology, Classification, Aspects of Durability. Proceed. Tenth Intern. Congress on the Chemistry of Cement, Göteborg, Sweden, p. 4iv 046-4iv 050 (1997).

[13] Davidovits, J. (ed.): Proceed. First European Conf. On Soft Minerallurgy "Geopolymer'88", Compiegne, (1988).

[14] Palomo, A. Grutzeck M.W. Blanco M.T. Alkali-activated fly ashes - A cement for the future. *Cement Concrete Res*. **1999**, 29, 1323-1329.

[15] Xu, H. van Deventer, J.S.J. Effect of Source Materials on geopolymerization. *Ind. Eng. Chem. Res.* **2003**, 42, 1698-1706.

[16] Rostovskaya, G. Illyin, V. Brodko, O. The investigation of Service Properties of the Slag Alkaline Concretes. Proceed. Intern. Symposium "Non-traditional Cement & Concrete", Brno, pp. 510-523, (2002).

[17] Vassilev, S.V. Baxter, D. Andersen, L.K. Vassileva, C.G. An overview of the composition and application of biomass ash. Part 1. Phase-mineral and chemical composition and classification. *Fuel*. **2013**, 105, 40-76.

[18] Jaworek, A. Czech, T. Sobczyk, A.T. Krupa, A. Properties of biomass vs. coal fly ashes deposited in electrostatic precipitator. *J. Electrostat*. **2013**, 71, 165-175.

[19] Toniolo, N. Boccaccini, A.R. Fly ash-based geopolymer containing added silicate waste. A review. *Ceram. Int*. **2017**, 43, 14545-14551.

[20] Alonso, M.M. Gascó, C. Martín-Morales, M. Suárez-Navarro, J.A. Zamorano, M. Puertas, F. Olive biomass ash as an alternative activator in geopolymer formation: A study of Strength, radiology and leaching behaviour. *Cement Concrete Comp*. **2019**, 104, 103384.

[21] Eliche-Quesada, D. Felipe-Sesé, M. Moreno-Molina, A. Franco, F. Infantes-Molina, A. Investigation of using bottom or fly pine-olive pruning ash to produce Environmental friendly ceramic Materials. *Appl. Clay Sci.* **2017**, 135, 333-346.

[22] Beltrán, M. Barbudo, A. Agrela, F. Jiménez, J. de Brito, J. Mechanical performance of bedding mortars made with olive biomass bottom ash. *Constr. Build. Mater*. **2016**, 112, 669-707.

[23] Pérez-Villarejo, L. Eliche-Quesada, D. Martín-Pascual, J. Martín-Morales M. Zamorano, M. Comparative study of the use of different biomass from olive grove in the manufacture of sustainable ceramic lightweight bricks. *Constr. Build. Mater*. **2020**, 231, 117103.

[24] UNE-EN 772-13. Test methods for masonry pieces. Determination of the absolute dry density and dry bulk density of parts for masonry factory (except natural stone), **2001**.

[25] ASTM C373 - Test method for water absorption, bulk density, apparent density, apparent porosity and apparent specific gravity of fired whiteware products. American Society for testing and Materials, **1994**.

[26] UNE-EN 772-1:2011. Methods of test for masonry units –Part 1: Determination of compressive Strength, **2011**.

[27] ISO 8302: 1991. Thermal insulation-determination of steady-state thermal resistance and related properties-guarded hot plate apparatus. International Standards Organization, Geneva, Switzerland, **1991**.

[28] García-Lodeiro, I. Palomo, A. Fernández-Jiménez, A. An overview of the chemistry of alkali-activated cement-based binders. In *Handbook of alkali-activated Cements, Mortars and Concretes*. 1st. ed.; F. Pacheco-Torgal, J.A. Labricha, C. Leonelli, A. Palomo and P. Chindraprasirt. Woodhead Publishing: Cambridge, UK, **2015**; pp. 19-43.

[29] Hajimohammadi, A. Provis, J.L. van Deventer, J.S.J. Time-resolved and spatially-resolved infrared spectroscopic observation of seeded nucleation controlling geopolymer gel formation. *J. Colloid Interf. Sci*. **2011**, 357,384-392.

[30]. Lee, W. K. W van Deventer, J. S. J. The effects of inorganic salt contamination on the strength and durability of geopolymers. Coll. Surf. A. **2002**, 211, 115-126.

[31] Rodríguez, E. Mejía de Gutiérrez, R. Bernal, S. Gordillo, M. Effect of the SiO_2/Al_2O_3 and Na_2O/SiO_2 ratios on the properties of geopolymers based on MK. *Rev. Fac. Ing. Univ. Antioquia*, **2009**, 49, 30-40.

[32] Sánchez de Rojas, M.I. Frías, M. The pozzolanic activity of different materials, its influence on the hydration heat in mortars. *Cem. Concr. Res*. **1996**, 26, 203-213.

[33] García-Lodeiro, I. Fernández-Jiménez, A. Palomo, A. Hydration kinetics in hybrid binders: Early reaction stages. *Cem. Concr Compos*. **2013**, 39, 82-92.

[34] García-Lodeiro, I. Fernández-Jiménez, A. Palomo, A. Macphee, D. Effect of calcium additions on N-A-S-H cementitious gels. *J. Am. Ceram. Soc*. **2010**, 93 (7), 1934-1940.

[35] Bernal, S.A. Rodríguez, E.D. Mejía de Gutiérrez, R. Provis, J.L. Delvasto, S.. Activation of metakaolin/slag blends using alkaline solutions based on chemically modified silica fume and rice husk ash. *Waste Biomass Valori.* **2011**, 3, 99-108.

[36] Kamhangrittirong, P. Suwanvitaya, P. Witayakul, W. Suwanvitaya, P. Chindaprasirt, P. Factors influence on shrinkage of high calcium fly ash geopolymer paste. *Adv. Mater. Res*. **2013**, 610-613, 2275-2281.

[37] Lloyd, R. Provis, J. Van Deventer, J. Microscopy and microanalysis of inorganic polymer cements. 2: the gel binder. *J. Mater. Sci*. **2009**, 44 (2), 620-631.

[38] Yip, C. Van Deventer, J. Microanalysis of calcium silicate hydrate gel formed within a geopolymeric binder. *J. Mater. Sci*. **2003**, 38, 18, 3851-3860.

[39] Palomo, A. Fernández-Jiménez, A. Kovalchuk, G. Ordoñez, L.M. Naranjo, M.C. OPC-fly ash cementitious systems: study of gel binders produced during alkaline hydration. *J. Mater. Sci*. **2007**, 42 (9), 2958-2966.